

An Investigation of Transition Metal Oxides in p-Type Dye-Sensitized Solar Cells

Undergraduate Honors Senior Thesis

Presented in Fulfillment of the Requirements for Honors Research Distinction in the
Undergraduate Chemical and Biomolecular Engineering School of The Ohio State University

By

Anna Dorfi, B.S

Chemical and Biomolecular Engineering

The Ohio State University

2014

Yiying Wu, Chemistry Research Advisor

ACKNOWLEDGMENTS

I would like to thank Dr. Yiyang Wu for his support and the opportunity to do research under his direction. I am also particularly grateful for the assistance given by Thomas Draskovic. He has helped and guided me from the very beginning of my research and has been a wonderful graduate research mentor. His willingness to give his time so generously has been very much appreciated.

INTRODUCTION

The field of alternative energies is becoming increasingly important as conventional fossil fuel sources are depleted, and the effects of global climate change are already being noted. In a society greatly dependent on energy production, the need for alternative and renewable energy forms is becoming a priority. Solar power is one of the most promising renewable energies, however it is still somewhat more expensive than conventional sources of energy and it has not yet been widely adopted [1]. In order for solar technologies to become a more viable energy option, its production needs to be scaled-up in an economically efficient way. Thus, research focused on low cost, high efficiency solar cells is necessary. It has been found that dye-sensitized solar cell technology is promising in terms of high cell efficiencies, and their ability to be manufactured from inexpensive materials [1]. Consequently, dye-sensitized solar cell (DSSC) research is at the forefront of these technologies and could provide a way to more efficiently capture solar energy for clean energy production.

In DSSCs light is absorbed by a sensitizer which is adhered to the surface of a wide band gap semiconductor. The charge separation takes place at the interface via photo-induced charge carrier injection from the dye into the semiconductor. The majority charge carriers are transported through the semiconductor to the charge collector. DSSCs are characterized by the nature of the semiconductor used. n-Type DSSCs (n-DSSC) use an n-type semiconductor (e.g. TiO_2 , ZnO). Electrons are injected into the conduction band by the photo-excited dye and diffuse to the external circuit. p-Type DSSCs (p-DSSC) use a p-type semiconductor (e.g. NiO). Holes are injected into the valence band by the photo-excited dye and diffuse to the external circuit. Research in Prof. Yiyang Wu's group has focused significantly on p-DSSCs, however performances continue to be much less than those of n-DSSCs. The inherent properties of NiO as

a semiconductor appear to be the source of these problems, and current research is focused on understanding the role of NiO as well as finding alternative semiconductors. While mainly the focus of research on supercapacitors, transition metal oxides similar to NiO, specifically manganese, cobalt, iron, and vanadium oxides, have not been thoroughly investigated for their use in p-DSSCs. Fundamental research on these 3d transition metal oxides is needed to understand their applicability and role in DSSCs.

BACKGROUND AND SIGNIFICANCE

Currently, nickel monoxide (NiO) is accepted as one of the few wide band-gap p-type semiconductors, and is a pale, light color. However, due to defects from oxidation during synthesis, it has been observed that the nickel oxidizes from 2^+ to 3^+ . This mixed oxidation state is likely the reason NiO actually appears to be black. It is known that the higher edge of the valence band in 3d metal oxides is heavily localized and holes created in the valence band are not easily transported through the semiconductor [2]. The holes are more localized on individual Ni atoms, due to their 3d orbital structure. It has been proposed that the holes are present as Ni^{3+} at the surface of NiO nanoparticles, and the charge transport involves hopping of charges at the NiO/electrolyte interface. Ultimately, if a NiO p-DSSC essentially functions due to this hole hopping mechanism induced by the oxidation of nickel by an excited dye molecule, then perhaps other metal oxides in the same 3d transition metal row with oxidation potentials similar to the Ni in NiO will work in p-DSSCs. These metal oxides should then theoretically function comparably to NiO in p-DSSCs.

The transition metal oxides that will be investigated are in the 3d row of the periodic table and exhibit many oxidation states, including 2^+ . Therefore, they have the potential to behave

similarly to NiO, where the metal surface is oxidized by the dye sensitizer and can participate in a redox reaction. The wide range of available oxidation states allows for easier oxidation of the metal oxide surface by the dye. The project aims to construct DSSCs with these various oxides, at varying oxidative states, in order to investigate their effectiveness for solar applications. When a photoactive dye is absorbed onto the transition metal oxide, redox reactions between the dye, electrolyte, and the oxide can be observed. A general equation that describes this aforementioned phenomenon is shown below as Equation 1:



A simplified mechanism that also shows how this DSSC works by a redox reaction can be seen below as Figure 1:

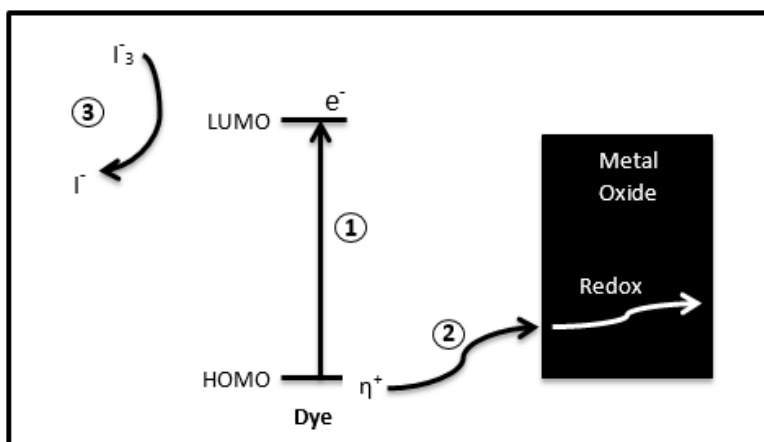


Figure 1: P-Type Dye-Sensitized Solar Cell Simplified Mechanism

This figure illustrates how a photoactive dye is excited by light energy and causes the electrons to become excited from the highest occupied molecular orbit (HOMO) level to the lowest occupied molecular orbit (LUMO) level. As mentioned before, the resulting positive charge from the redox reaction, called the hole, is injected into the metal oxide which ultimately creates a current through the semiconductor to the external circuit.

The significance of this project is the emphasis on the investigation of using relatively low cost transition metal oxides made from metals in the 3d row of the periodic table, such as: Manganese, Cobalt, Iron, and Vanadium in DSSCs. Fundamental research on transition metals and their applicability for DSSCs has not been extensively explored. Again, the wide range of oxidative states possible for these transition metal oxides makes them viable candidates, due to the oxidation reactions that can occur from the excitation of an absorbed photoactive dye sensitizer. The solar cells that are constructed for this project use a non-aqueous electrolyte solution composed of the I^-/I_3^- redox couple. Research has shown that non-aqueous electrolyte solutions achieve higher cell potentials than aqueous electrolytes, due to their ability to encompass wider voltage windows and liquid ranges, thus leading to higher possible solar cell efficiencies [3]. Specifically, the aforementioned transition metal oxides will be used in preliminary constructions of non-aqueous DSSCs and their efficiencies will be compared to existing technologies.

EXPERIMENTAL METHODOLOGY

Preliminary Oxides Methodology. The transition metal oxides of manganese, cobalt, iron, and vanadium were synthesized via a modification of a previously developed sol-gel method for synthesizing NiO thin films [4]. For each desired oxide, 7.72×10^{-3} moles of a soluble metal salt precursor ($Mn(NO_3)_3$, $Co(NO_3)_3$, $Fe(NO_3)_3$, or $VO(SO_4)$) was combined with 1 g of distilled water, 3 g of ethanol, and 1 g of F108 polymer. The polymer was added to the solution to act as a template for the oxide film formation and so that the film adheres to the substrates. The metal salt polymer solution was then left to settle over three days. If any solids precipitated out, then the solution was centrifuged and the resulting supernatant solution was kept. This was the precursor solution used to make the metal oxide films.

Syntheses of Transition Metal Oxides with 2⁺ Oxidation States. Syntheses for the formation of pure nano-scale lower oxidative transition metal oxides; specifically CoO and MnO were found and used in order to have a direct comparison to NiO. All syntheses used to produce these compounds were solvothermal methods and produced nanoparticles. The synthesis of CoO consisted of combining cobalt acetate, ethanol and polyethylene glycols 4000 in an autoclave at 150 °C for 24 hours [5]. The resulting precipitate was washed with ethanol several times and filtered by centrifugation before drying at room temperature. The resulting CoO precipitate was dark blue. The dark brown MnO product was prepared similarly to the CoO product. In a glove box, manganese acetate and ethanol were combined and transferred to a Teflon-lined stainless steel autoclave. The autoclave was heated at 200 °C for 24 hours. The product was washed with water and ethanol several times and filtered by centrifugation. The final washed MnO product was then dried at 80 °C for 6 hours in a vacuum [6].

n-Type Semiconductors for Sensitized Photocathodes. It was attempted to replicate the tin-doped indium oxide (ITO) results found from the lab group by creating small area films from commercial ITO nanoparticle powder (NanoTek®, Alfa Aesar) suspended in ethanol. The Fe₂O₃ was synthesized using the aforementioned NiO sol-gel modification. WO₃ was synthesized according to previous literature reports [7]. A solvothermal synthesis used sodium tungstate dehydrate dissolved in water. 2M HCL was added until the pH was 5 and it was then submerged in a water bath at 80°C for four days. The resulting precipitate was washed and filtered by centrifugation with distilled water various times. It was dried in the oven at 160°C for two hours.

Film and Cell Preparation. The general method for preparing films involved doctor-blading a solution that contained the desired transition metal on a fluorine-doped tin oxide (FTO) glass slide and then annealing the film at a high temperature. For the preliminary oxides, FTO slides

were cleaned and their conductive sides were marked for future use. Each slide was taped off to form a “square well” area (around 1.3 mm² for larger test films and around 0.5 mm² for small films) in the middle. 50 µL of each metal solution were deposited above the marked area, and a microscope slide was used to doctor blade the film evenly. The solution was let dry for ten minutes. The resulting film thicknesses ranged around two micrometers and were not less than a micrometer thick. The thin film doctor blading technique was altered to ensure this standard. The tape was then removed and the glass plates were put separately in an oven at three different temperatures: 250 °C, 350 °C, and 450 °C.

Similarly for CoO, MnO, ITO and WO₃, a solution of ethanol and their respective dry nanoparticle powders were combined and sonicated for forty minutes to form a paste of comparable viscosity to the sol-gel pastes. These pastes were then used to create films via the doctor blading method previously described. All of the prepared CoO, MnO, ITO and WO₃ films were then annealed in a tube furnace under argon atmosphere at 450 °C at a heating rate of 2.5 °C/min and held for 30 minutes, in order to prevent further oxidation.

The film plates were then either sensitized or left bare for comparison studies. The sensitization was accomplished by immersing the films in a dye-sensitizer for 15 hours to ensure sufficient dye loading. The DSSCs were then assembled by placing a platinum-coated conducting FTO glass plate with a hole drilled into it on the dye-sensitized film electrode. These electrodes were joined using a 60 µm polymer spacer (Solaronix SA, Switzerland) that was sealed first by heating at 120 °C for 5 minutes. An electrolyte was made with 1.0 M LiI and 0.1 M I₂ in dry methoxypropionitrile and it was injected into the cell via vacuum backfilling through the drilled hole. The hole was then sealed using the polymer film adhesive, a thin glass cover slide and a quick-dry sealant.

Characterization. For the preliminary oxides, each metal film annealed at the various temperatures was analyzed using x-ray powder diffraction (XRD, Rigaku) to confirm what oxidative species were formed at the three temperatures and to determine at which temperature each species needed to be annealed. Once the metal oxides films were made and characterized by x-ray powder diffraction, their electrochemical properties were then evaluated using cyclic voltammetry in a 0.01 M LiI, 0.001 M I₂, and 0.1 M LiClO₄ methoxypropionitrile electrolyte and compared to the results obtained for the original NiO films. Cyclic Voltammetry (CV) is an electrochemical test that ramps the potential of a working electrode against a reference electrode for a certain range. The potential is ramped first in the negative direction and then backwards in the positive direction. If there is any redox activity within the desired potential range, peaks can be observed which account for the oxidation (peaks with positive currents) and reduction (peaks with negative currents) activity of the material being tested. These tests allow each metal oxide to be compared to NiO and its redox activity, so that conclusions can be drawn to how they will perform when tested as a solar cell. Linear sweep voltammetry was used to test the solar cell performances both in dark and under illumination from 1 sun AM 1.5G simulated sunlight (Small-Area Class-B Solar Simulator, PV Measurements). Electrochemical data was collected using a Gamry Instruments Reference 600. All potentials are reported with respect to the I⁻/I₃⁻ redox couple.

RESULTS AND DISCUSSION

Preliminary Transition Metal Oxide Testing. Relatively pure phase oxides of each transition metal were obtained at various film annealing temperatures: Mn₃O₄/Mn₂O₃ mixture was confirmed at 450 °C, Co₃O₄ at 350 °C, Fe₂O₃ at 450 °C, and V₂O₅ at 450 °C. Their XRD results can be seen in Appendix as Figures A1-A4. The oxides synthesized using the NiO sol-gel paper

adaptation were not directly comparable to Ni (II) as the states present for the cations in each metal oxide were Manganese (III/IV), Cobalt (III/IV), Iron (III), and Vanadium (V). When analyzing the CV's of the preliminary oxides it is evident that they do not follow a similar CV shape or activity to NiO. The CV's of the preliminary metal oxides produced can be seen in Appendix B as Figures B1-B4. This was to be expected, however, as these metal oxides are all of higher oxidative states (III-V) than Ni (II) and likely do not have a similar charge hopping mechanism. Linear sweep voltammetry tests were then done once the solar cells were assembled in order to obtain the maximum current and voltage obtainable from a DSSC made of each oxide. The first cells made were unsensitized and the metal oxide films were left bare. This was done in order to see how the metal oxide itself acted in the DSSC. From the preliminary unsensitized tests it is interesting to note that Fe_2O_3 exhibited anodic current when compared to the other common oxides produced. Mn_3O_4 exhibited slight anodic current but the overall results show that these common metal oxides produced did not exhibit any cathodic photocurrent on their own. Thus, the DSSC photocurrent results of the sensitized cells were all due to the photo-excitation of the sensitizer. A ruthenium-based dye was used for these sensitized cell tests. The unsensitized results are shown below as Figure 2:

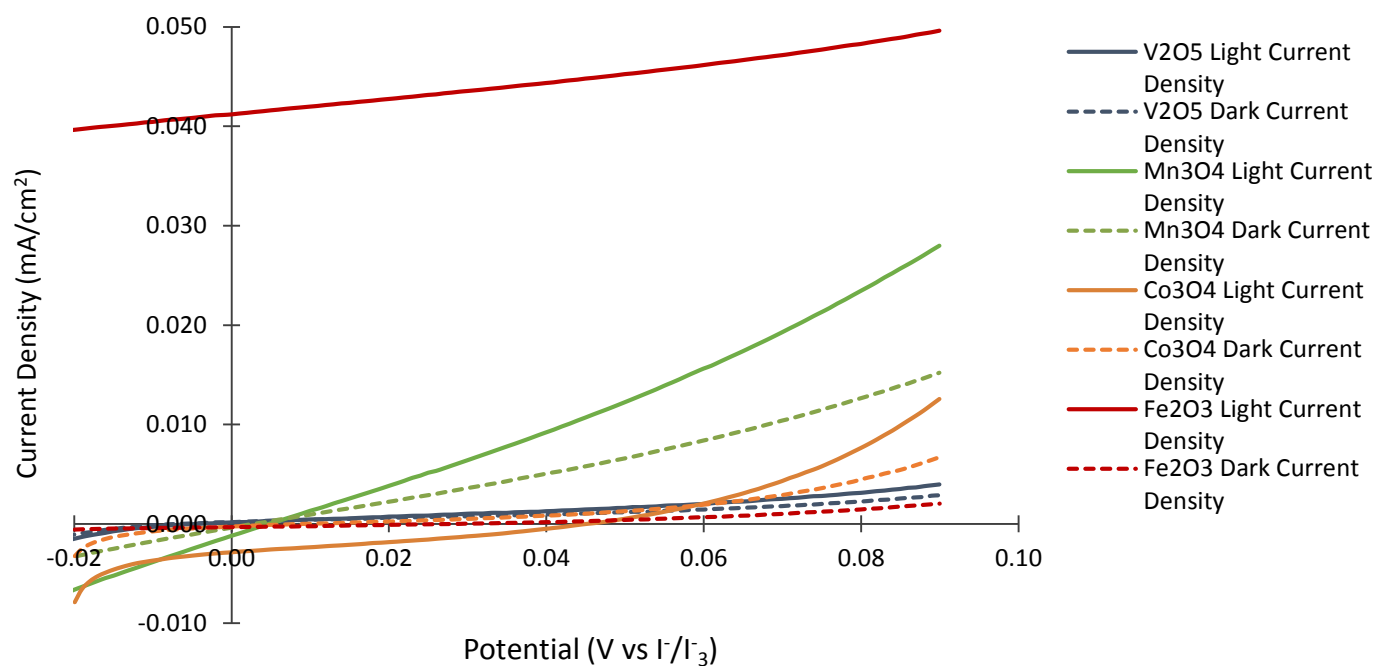


Figure 2: Non-sensitized DSSC results from metal oxides synthesized using NiO synthesis modification

Using a ruthenium based dye, referred to as O3, solar cell tests were done in order to determine the highest short circuit current (I_{sc} , when the voltage is zero) and the highest open circuit voltages (V_{oc} , when the current is zero) produced by each cell. A graph of these results can be seen below as Figure 3:

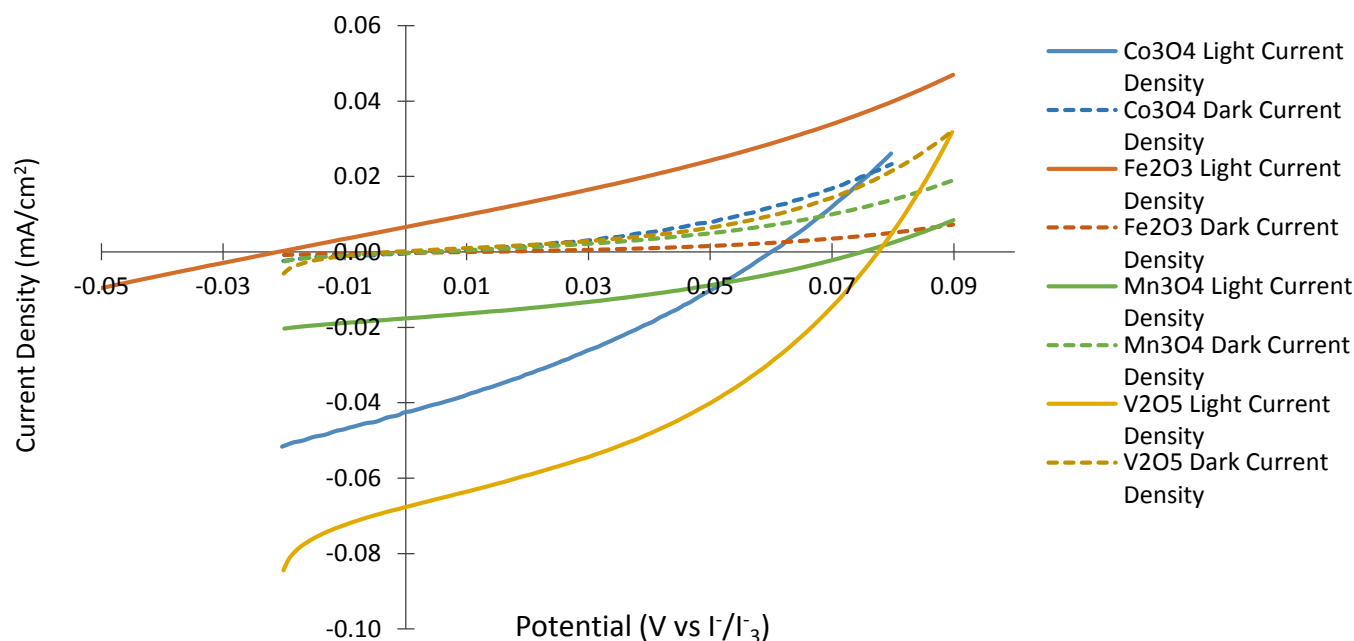


Figure 3: Comparison of Metal Oxides synthesized from NiO synthesis modification in O3 dye

The highest V_{oc} 's were 77.7 mV for V_2O_5 and 74 mV for Mn_3O_4 . The highest I_{sc} densities (which take into account the area of the films) were -0.0674 mA/cm^2 for V_2O_5 and around -0.042 mA/cm^2 for Co_3O_4 . Even though V_2O_5 performed the best out of all the other oxides (highest I_{sc} and V_{oc}), it was observed to undergo a color change from yellow to light green when it came in contact with the $I^-/I_2/LiClO_4$ electrolyte. It was then determined to be unstable in the electrolyte used for this study and no further investigation in regards to other vanadium oxides was done. Vanadium (IV) is dark blue, so the combination of IV/V oxidation states could suggest that the electrolyte was actually reducing the V_2O_5 film. Further research could be done with vanadium oxides in differing electrolytes, but for the scope of this study it was not considered for further testing. These results, however, when compared to the NiO results in the same O3 ruthenium-based dye show that the currents and voltages produced are negligible. The graph comparing the results to NiO data is shown below as Figure 4:

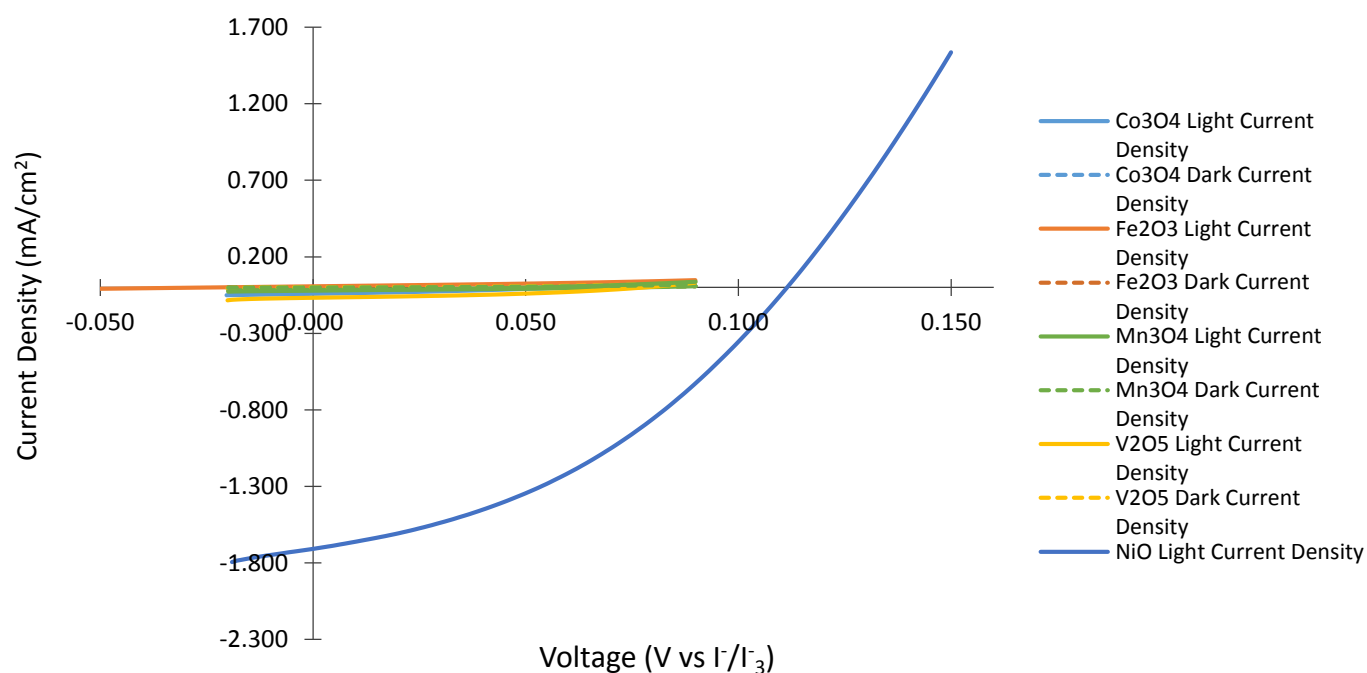


Figure 4: Comparison with NiO in O3 dye of Metal Oxides synthesized from NiO synthesis modification.

This synthetic method was a starting point for the investigation but did not produce the monoxides desired to directly compare to NiO. The overall aim was then to vary the procedure by which the metal oxides were made, in order to produce metal oxide films of the 2^+ state so they could be directly compared to Ni^{2+} . Further research was then done to find various metal oxide syntheses for lower metal oxide oxidative states. Syntheses were found for CoO and MnO and their results are discussed in the following section.

Cobalt and Manganese Monoxide Investigation. CoO and MnO were also confirmed using XRD (Rigaku) and be seen in Appendix A as Figures A5-A6, respectively. Due to the low oxidation state in the monoxides, cobalt and manganese could easily be oxidized to 3^+ during the synthesis or film preparation. XRD shows there was some amount of Co_3O_4 and Mn_3O_4 in the products, but it is believed that the monoxides were the dominant phase. Preliminary CV tests of CoO and

MnO were done to compare to NiO's results in order to determine their possible performance as DSSCs. The CVs for CoO and MnO are seen below as Figure 5 and Figure 6, respectively:

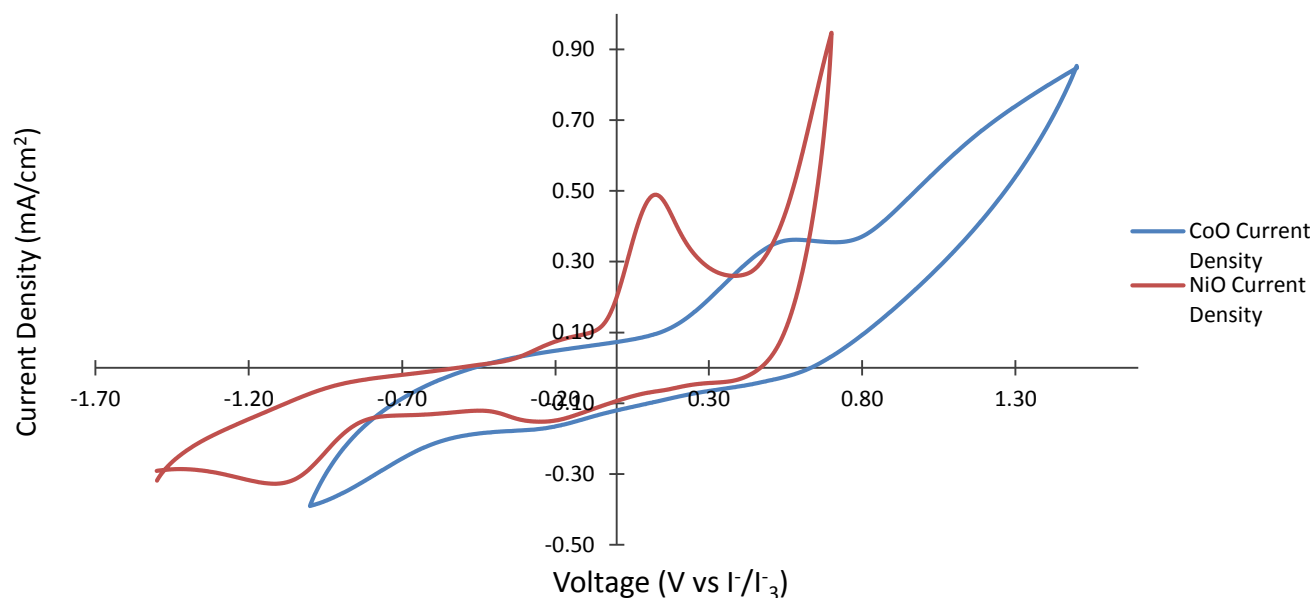


Figure 5: CV of CoO (scan rate = 50 mV/s)

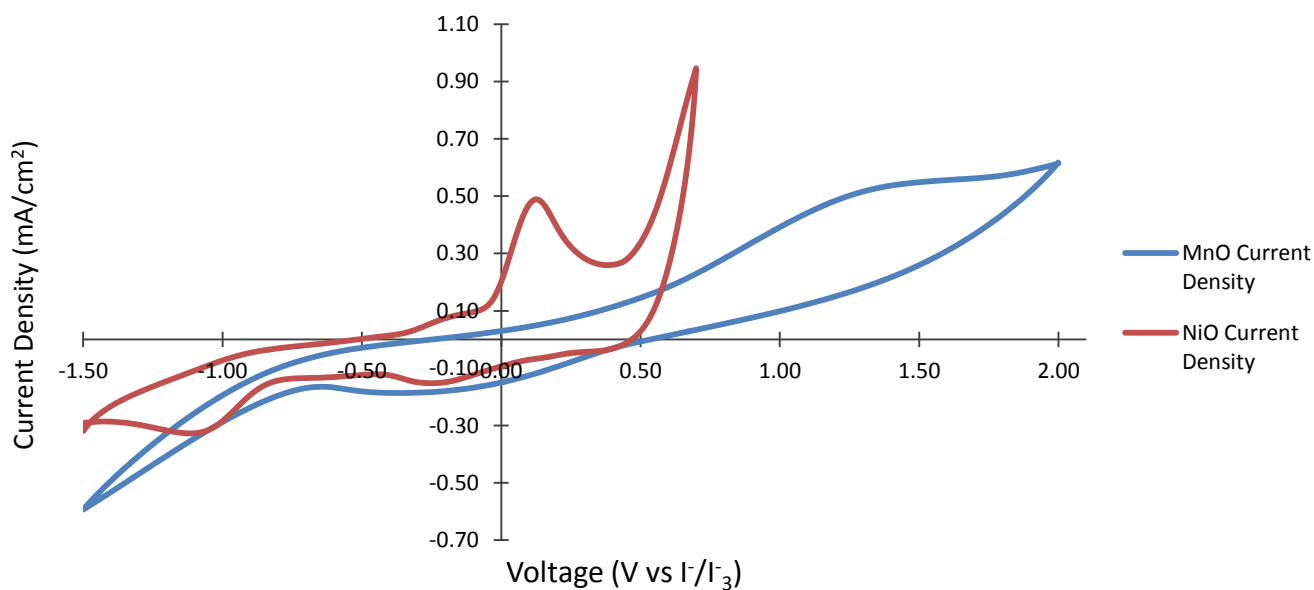


Figure 6: CV of MnO (scan rate = 50 mV/s)

Typically, the open-circuit voltage of a p-DSSC is determined by the potential of the valence band edge with respect to the redox couple in the electrolyte. However, due to the localized nature of the charge carriers, as discussed before, the V_{oc} for NiO or similar oxides can be viewed as the oxidation potential of the metal species with respect to the electrolyte.

From the CV's it can be seen that the oxidative peaks for both CoO and MnO are slightly more positively shifted than the oxidative peak for NiO and occur at a higher potential. This should then directly correlate to a higher V_{oc} than NiO for both CoO and MnO, with MnO having the highest V_{oc} . The shape of the CV's for both monoxides are similar to that of NiO so it is expected that their solar cell linear sweep voltammetry tests should yield comparable results to NiO. Small area films of both CoO and MnO were then made into both un-sensitized and sensitized cells and their performances were tested in both light and dark conditions. The unsensitized DSSC results are shown in Figure 7 below and a clear view of the sensitized results are shown in Figure 8. These results were then compared to NiO, as seen in Figure 9.

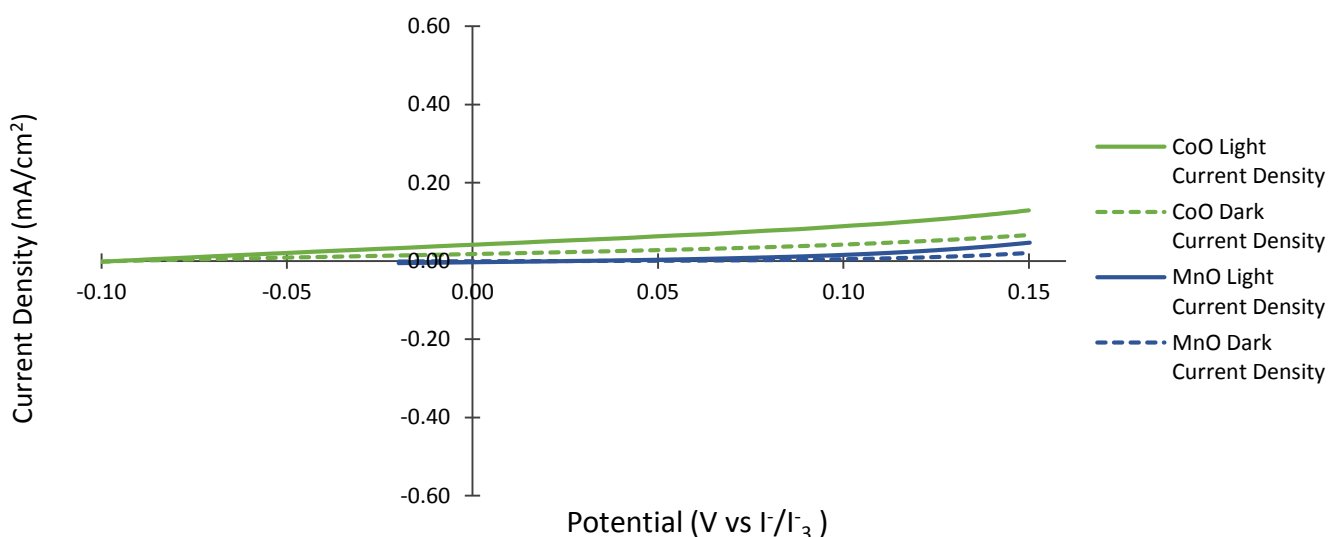


Figure 7: CoO and MnO Unsensitized Cell Performances

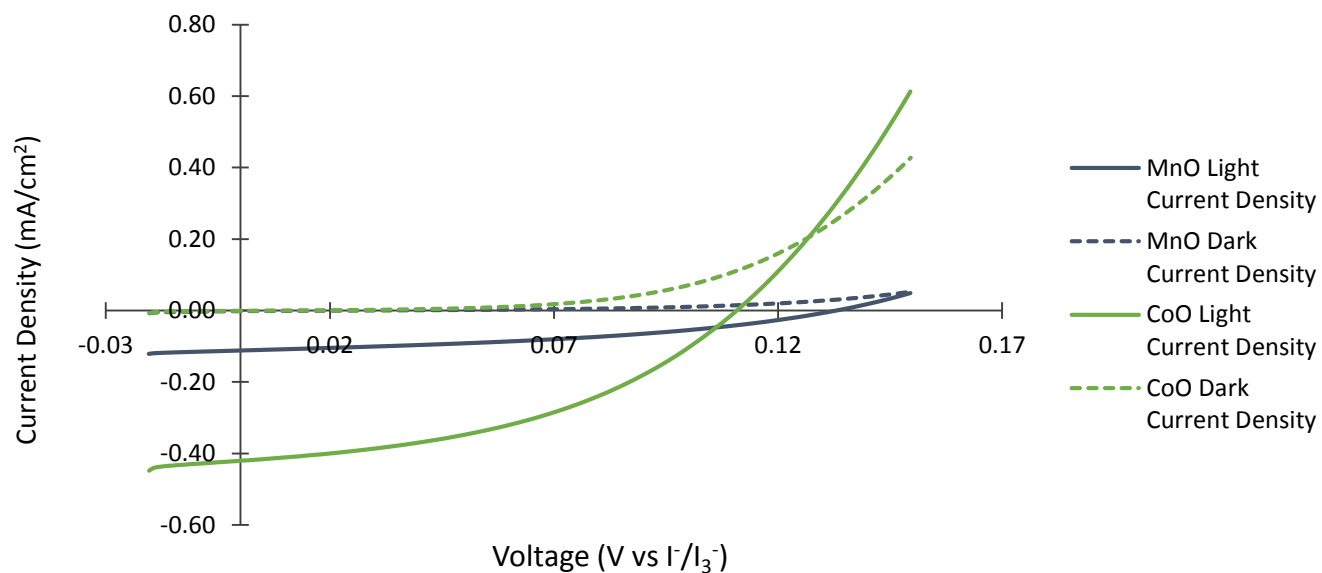


Figure 8: CoO and MnO DSSC Results in O18 dye

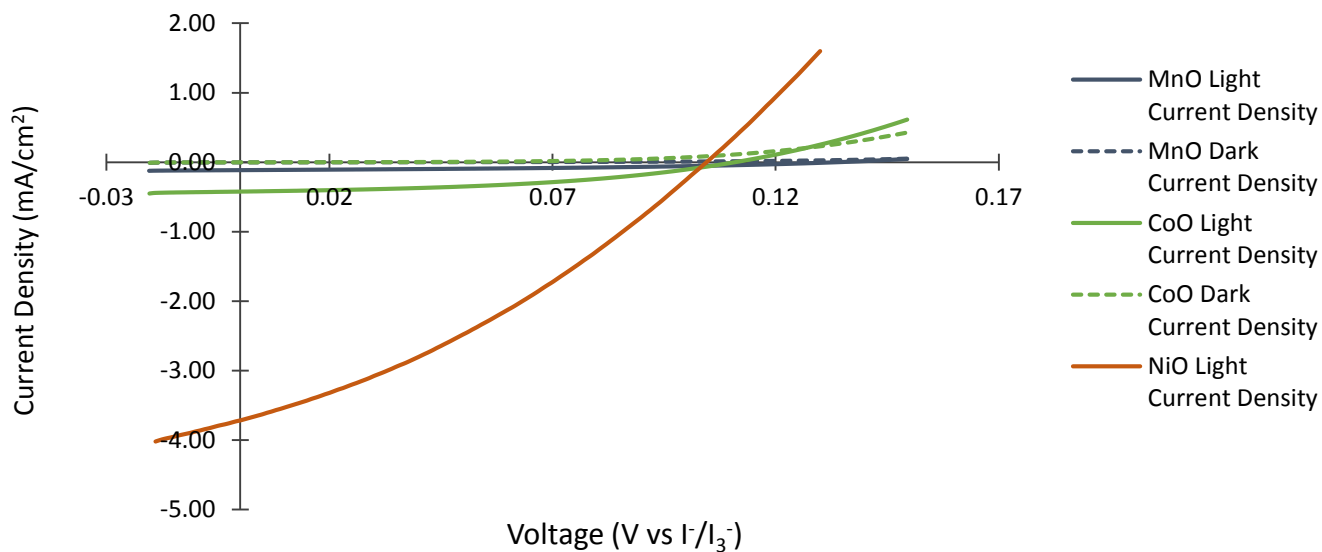


Figure 9: CoO and MnO DSSC Results in O18 dye in comparison to NiO

The unsensitized DSSC results show that both CoO and MnO exhibit negligible photocurrent themselves. They are slightly anodic and so they would only be marginally inhibiting the photocurrent produced from the sensitized DSSC, but it can be safely interpreted that no cathodic current produced from the sensitized DSSC is due to the metal oxides themselves. When analyzing Figure 9 it was determined that the predicted trend from the CV's oxidative peaks did support the trend seen in the DSSC results. This also helps support the hypothesis that the original mechanism for NiO p-DSSCs is also present in CoO and MnO DSSCs. The cathodic current generated is due to the hopping mechanism of holes from the oxidation of the monoxide cation from 2^+ to 3^+ . The V_{oc} for NiO was 104 mV compared to the highest V_{oc} of 135 mV for MnO ($I_{sc} = -0.112 \text{ mA/cm}^2$) that was followed CoO with a V_{oc} 112mV. The highest I_{sc} density was -0.42 mA/cm^2 for CoO when comparing only CoO and MnO. However, when analyzing the highest current densities achieved in comparison to NiO's I_{sc} of -3.49 mA/cm^2 , Figure 9 shows that the currents are not comparable to NiO's maximum current density.

A further literature review was done in order to explain the discrepancy in current density between the three monoxides. It was determined that the size of the cation decreases from manganese to nickel and more oxygen overlap takes place in the metal-oxide of NiO compared to MnO. This increased overlap of metal 3d and oxygen 2p orbitals correlates to higher hole mobility as well as easier hopping [8]. This explains the slower hole mobility seen in MnO and CoO, as the trends in the I_{sc} results follow the aforementioned trend as well. Slower mobility increases the probability for a hole in the metal oxide to interact with electrolyte and become reduced, thus inhibiting the maximum current achievable in the DSSC. Furthermore, when examining the 3d orbital configuration of the monoxides, it was determined that Co changes

from a high spin 2^+ state to a low spin 3^+ state. This also correlates to slow hole mobility and hole hopping, as the change in spin inhibits this mechanism. This occurrence can be seen below as Figure 10:

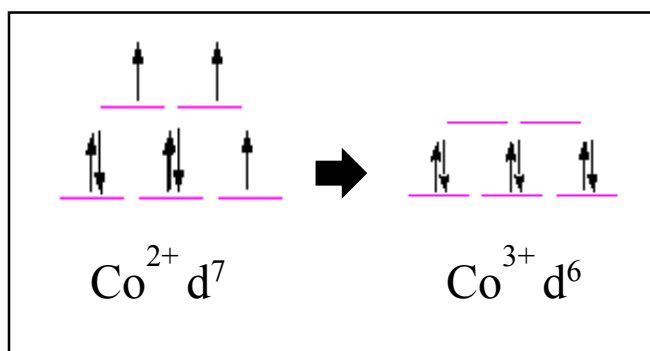


Figure 10: Cobalt d-orbital Configuration

Similarly, the oxidation from Mn^{2+} to Mn^{3+} results in a Jahn-Teller distortion in the MnO structure. This phenomenon occurs frequently in d^4 orbital configurations, which is the state Mn (II) is oxidized to and becomes Mn (III). The ligands (oxygen) attached to the Manganese atoms are stretched in the z-direction and have also shown to severely inhibit hole mobility [9]. This depicted in Figure 11 below:

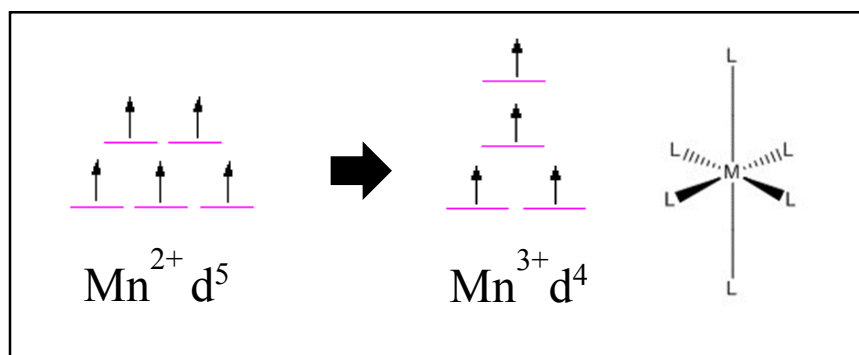


Figure 11: Manganese d-orbital configuration [9]

Lastly, when the d-orbital configurations for CoO and MnO are compared to NiO it can be determined that when Ni (II) oxidizes to Ni (III) there is no significant chemical environmental change for the monoxide. Only one electron is lost during the process but there are no spin changes or deformations to the structure. This is clearly seen in Figure 12 below:

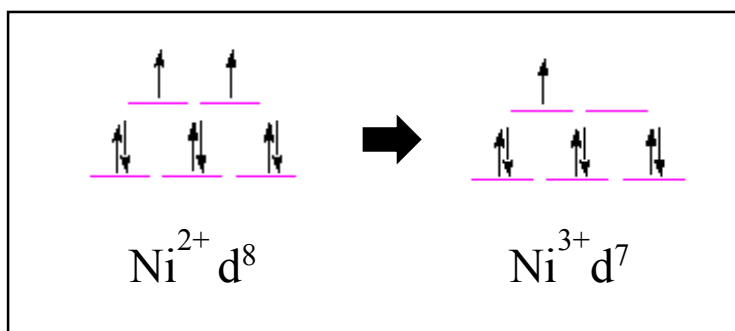


Figure 12: Ni d-orbital configuration

Use of n-Type Semiconductors in p-DSSCs. During the transition metal monoxide study, Prof. Wu's lab group, out of curiosity, had begun testing tin-doped indium oxide (ITO) as a possible semiconductor for use in p-DSSCs in order to see if cathodic current would be produced, as ITO is typically an n-Type semiconductor. ITO is also usually used as a coating for the glass plates used in DSSC construction. They were able to achieve a relatively high cathodic short circuit current density that was comparable to NiO. The hypothesized mechanism by which this cell works is shown below as Figure 13:

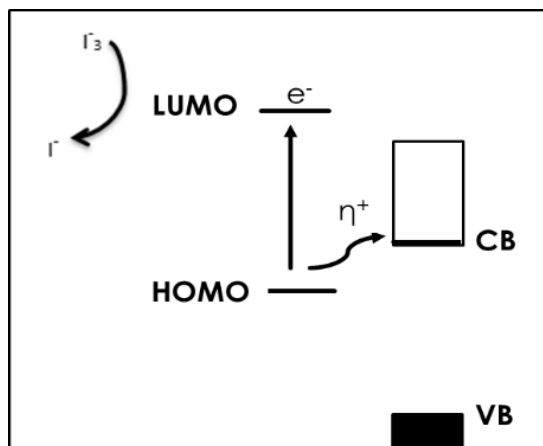


Figure 13: Mechanism for ITO DSSC

There is cathodic current generated, even though ITO is an n-type semiconductor, because there is hole injection into the conduction band of the ITO, rather than injection into the valence band for a p-Type semiconductor. This is a very interesting mechanism so further research was done in order to find other metal oxides with a similar conduction band position to ITO. Figure 14 below shows various metal oxides and their band gap positions.

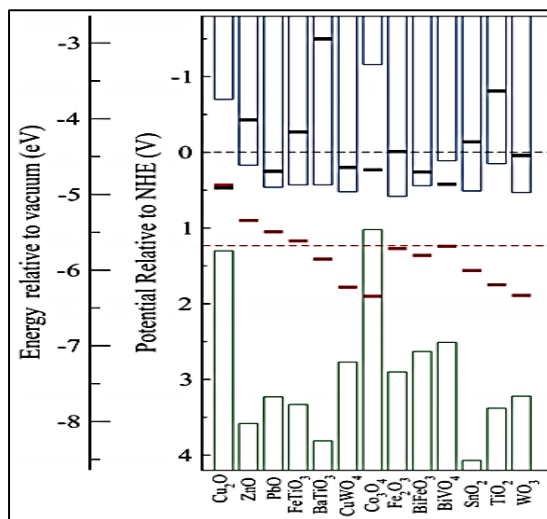


Figure 14: Conduction band positions of various metal oxides [10].

This figure shows that tungsten oxide (WO_3) and iron (III) oxide (Fe_2O_3) have similar conduction band positions to tin oxide (SnO_2) and so they would be interesting to synthesize for

further testing and comparison to ITO's performance. Sensitized ITO cells with ruthenium O3 dye were assembled and tested in order to validate the previous results achieved by the lab group. These results can be seen below as Figure 15:

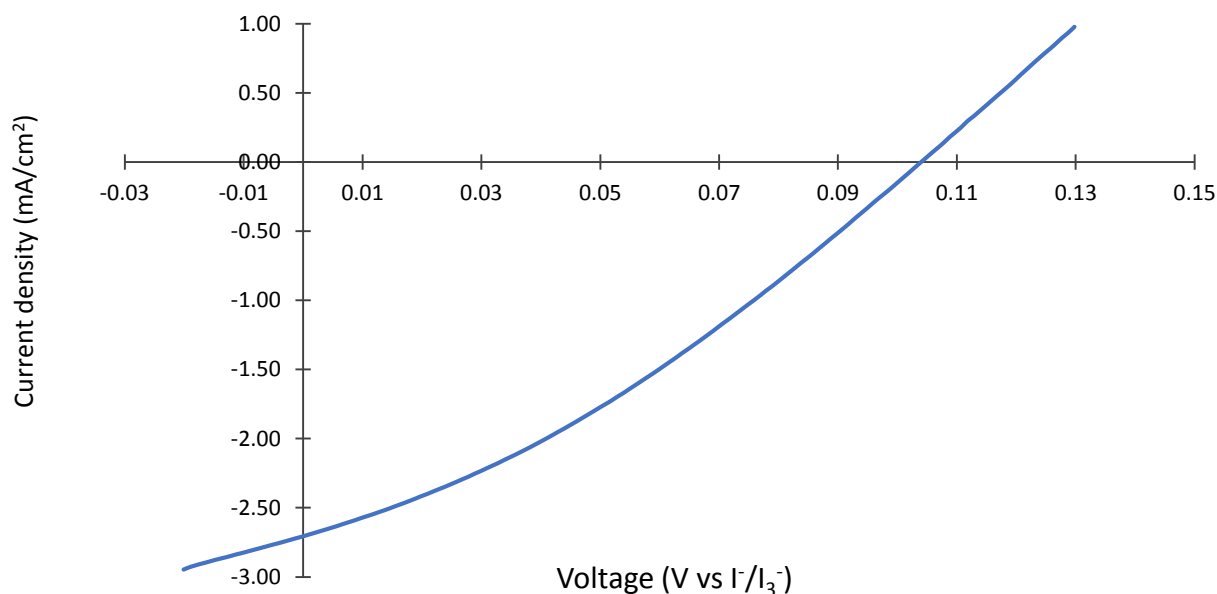


Figure 15: O3 Dye DSSC ITO Results under Light

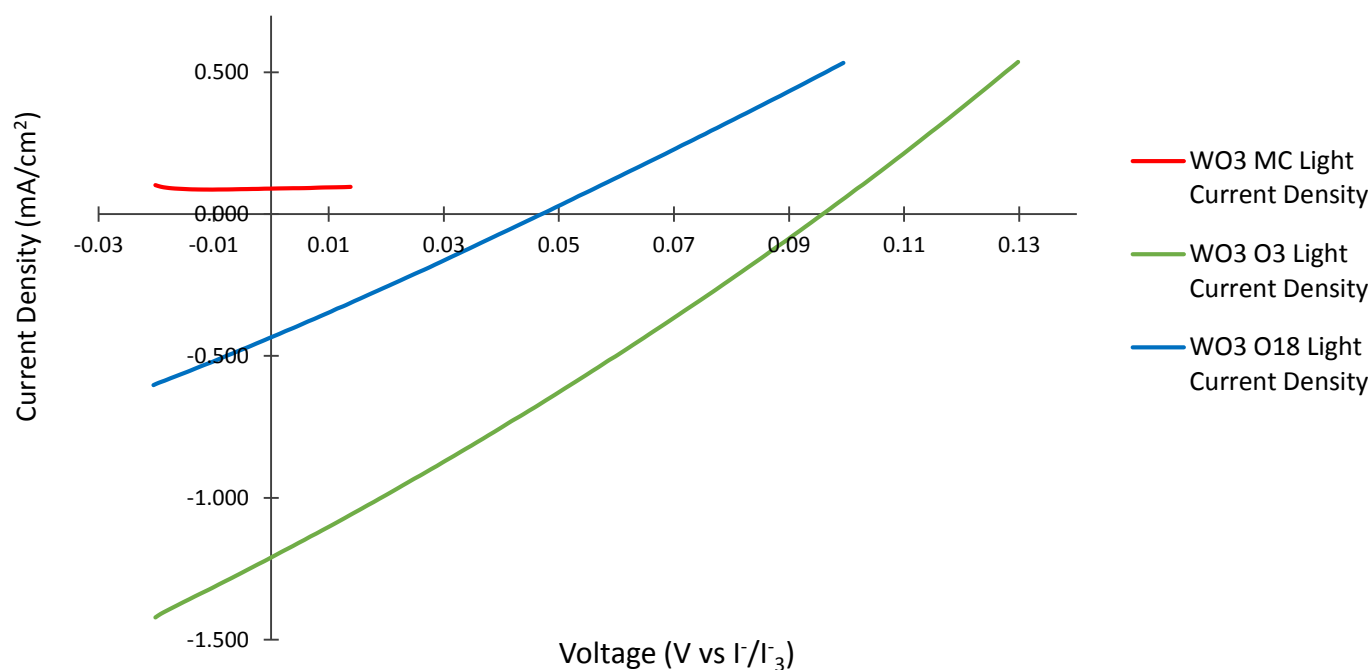
The I_{sc} of the ITO cells is high compared to the monoxides but still slightly less than the NiO results. The highest I_{sc} density achieved was -2.69 mA/cm^2 in O3 dye with a V_{oc} of 104 mV. However, the I_{sc} is still promising and can be further improved. ITO showed the most promising performance when compared to NiO and so the transition metals with similar conduction band positions were also tested with dyes of various reductive potentials in order to analyze which dye sensitizers maximized their performances. Two Ruthenium based dyes, O3 and O18, were used as well as an organic dye referred to as “MC” [11, 12]. The reduction potentials of the dyes are shown below in Table 1:

Table 1: Reduction Potentials of Dye Sensitizers

Dye Type	Reduction Potentials
O18	0.106 V
O3	0.136 V
PMI-T2-TPA “MC”	1.046 V

DSSC's of both WO_3 and Fe_2O_3 were then constructed and tested with various dye sensitizers.

The results for WO_3 can be seen below as Figure 16:

**Figure 16:** WO₃ DSSC Results for various dyes

The highest I_{sc} density was -1.20 mA/cm^2 in O3 dye and the maximum V_{oc} was 96.8mV.

However, the O18 dye did not perform as similarly to the O3 dye. This could be due to poor dye

loading or due to the fact that the O18 dye may have been old and somewhat degraded compared to the freshly synthesized O3 dye that was tested. However, these results are more interesting in regards to the organic dye performance. The organic dye produced anodic current rather than the cathodic current produced for the ruthenium based dyes. This may be due to “MC”’s high reduction potential which could be at a position too far into the band gap of WO_3 . Referring to Figure 16, this seems like a plausible explanation, as the reduction potential of 1.046V falls in the wide band gap of WO_3 . The lack of charge carrier density in that region would account for the poor performance with the organic “MC” dye. This should be expected for Fe_2O_3 as well. The results for Fe_2O_3 are seen below as Figure 17:

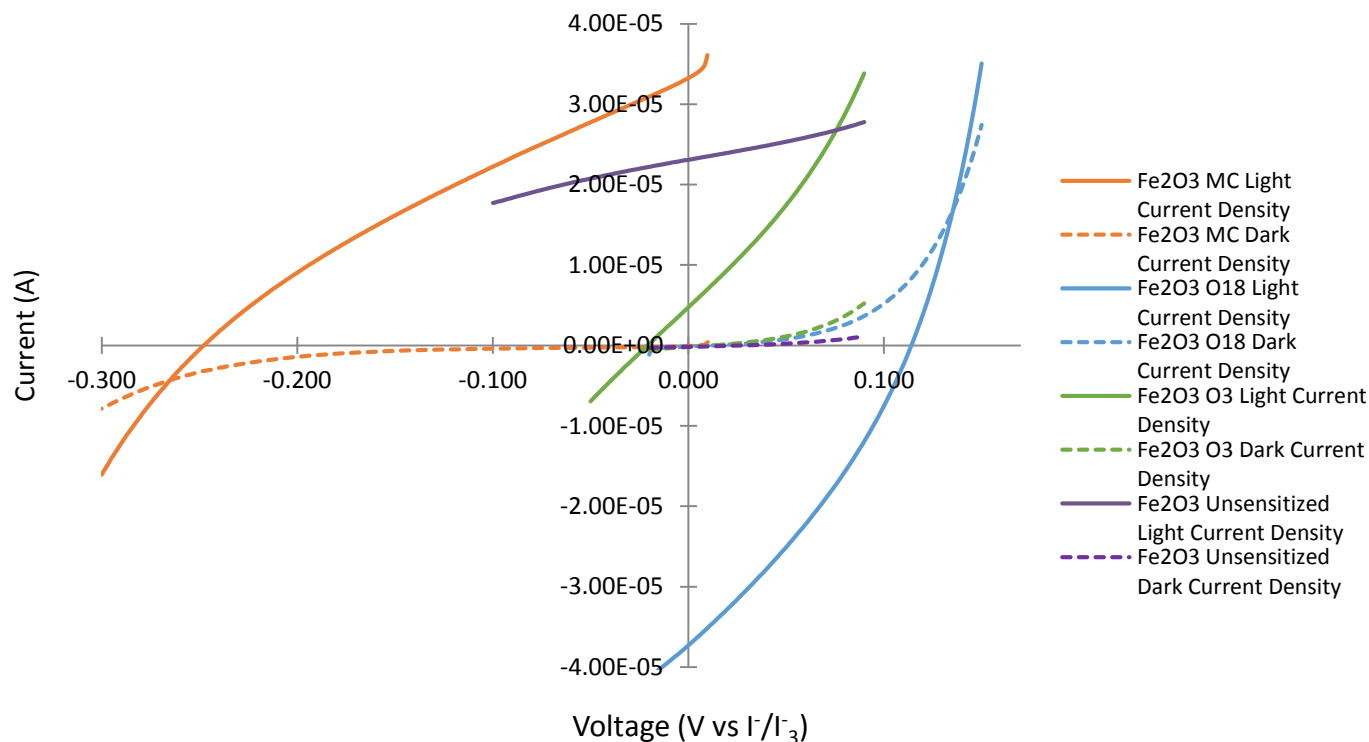


Figure 17: Fe_2O_3 DSSC Results for various dyes

As stated in a previous section, Fe_2O_3 exhibited anodic current when assembled into an unsensitized DSSC. The organic “MC” dye enhanced Fe_2O_3 ’s anodic current, most likely due to the same reason it produced anodic current with WO_3 (its reduction potential is in the band gap of the metal oxide). The O3 dye, however, produced negligible cathodic current. This may be due to the fact that the dye is balancing out the intrinsic anodic character of the Fe_2O_3 , because both the O3 and Fe_2O_3 are orange in color and could be competing for the same light absorption. The O18 dye, on the other hand, is almost black and very dark in color. That would explain its better performance with Fe_2O_3 , although the current produced is still negligible in comparison to ITO, WO_3 , and NiO.

CONCLUSIONS

Preliminary Transition Metal Oxide Tests. The short-circuit currents of the preliminary oxides created using the NiO sol-gel modification were barely visible on the same scale with NiO’s results. The open-circuit voltages were also significantly lower for every oxide in comparison to NiO. However, no preliminary oxides created using this method were monoxides and thus did not fit into the original hypothesis that directly compared the Ni (II) state. These results were not useful for further analysis or investigation and further research was done to synthesize monoxides of the transition metals in the 3d row that were similar to NiO, such as CoO and MnO.

Cobalt and Manganese Monoxide Investigation. The highest V_{oc} was for MnO and the lowest was for NiO. This follows the trend shown by the CV tests, however the currents exhibited by CoO and MnO are still essentially negligible in comparison to the NiO results. This discrepancy was found to be due to the spin change from high spin to low spin that occurs when Co is

oxidized from 2^+ to 3^+ . This change accounts for low hole mobility. Subsequently, when Mn is oxidized from 2^+ to 3^+ it changes to a $d4$ configuration and metals in $d4$ configurations are more susceptible to Jahn Teller distortions. This Jahn Teller distortion also correlates to a significant decrease in the hole mobility of the oxide. However, when NiO undergoes oxidation there is no significant change to the chemical or physical environment of the oxide and so there is no impact to the hole mobility of NiO, thus it outperforms CoO and MnO.

n-Type Semiconductors in p-DSSCs. The ITO and WO_3 results seem to be the most promising for future research in regards to p-DSSC research, as preliminary testing resulted in more than double the magnitude of the I_{sc} than compared to the I_{sc} of the monoxides CoO and MnO. When comparing the performances of the ruthenium-based dye sensitizers to the organic dye sensitizer it was concluded that the organic dye HOMO reduction potential was too low into the band gap of these oxides, thus there was very little to no charge carrier density available for WO_3 and Fe_2O_3 . The organic “MC” dye produced anodic current for both WO_3 and Fe_2O_3 . It was also interesting to note that the ruthenium O3 dye produced negligible cathodic current when tested with Fe_2O_3 due to the competing light absorption of the dye with the metal oxide of similar color. Optimizing the film thickness, uniformity, as well as the ruthenium based dyes used can further increase the WO_3 and ITO performances.

FUTURE WORK

Although WO_3 did not produce results in a similar range to ITO or NiO, it shows promise for improvement. The I_{sc} produced was still double the magnitude of the I_{sc} for CoO and MnO. The ITO is also a heavily doped semiconductor and doping WO_3 should be done to increase the electron density of the Fermi level near the conduction band, which is higher for ITO than WO_3 ,

due to the doping by tin. Similarly, a complete study of the 3d transition metal monoxides should be done to compile a complete understanding of these monoxides, as well as compare their performances to the more widely studied NiO. Thus, the next step in this investigation would be to synthesize FeO and assemble DSSCs for comparison to CoO, MnO, and NiO. What is particularly interesting about FeO is that there is no geometry distortion or change in spin when it undergoes oxidation from 2^+ to 3^+ , as seen in the d-orbital configurations. It is high spin for both the 2^+ and 3^+ states. Thus, charge transport may occur more similarly to NiO. The d-orbital configuration for FeO is shown below in Figure 18:

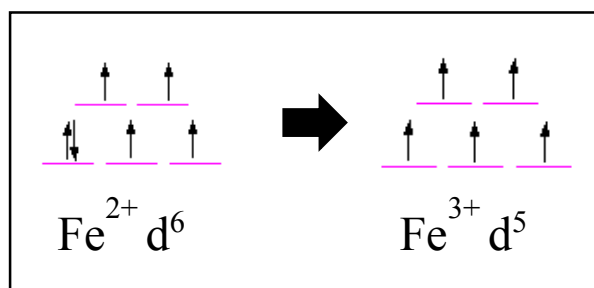


Figure 18: Iron d-orbital configuration

REFERENCES

1. Ecole Polytechnique Fédérale de Lausanne. "Dye-sensitized solar cells rival conventional cell efficiency." *Science Daily*. 10. Jul. 2013. Web. 21. Jul. 2013. <
<http://www.sciencedaily.com/releases/2013/07/130710141850.htm>>
2. Natu, Gayatri, Panitat Hasin, Zhongjie Huang, Zhiqiang Ji, Mingfu He, and Yiyang Wu. "Valence Band-Edge Engineering of Nickel Oxide Nanoparticles via Cobalt Doping for Application in P-Type Dye-Sensitized Solar Cells." *ACS Applied Materials & Interfaces* 4.11 (2012): 5922-929. Print.

3. Gores, Heiner J., and Hans-Georg Schweiger. "Non-Aqueous Electrolyte Solutions." Non-Aqueous Electrolyte Solutions. Ed. Robert F. Savinell, Ken-ichiro Ota, and Gerhard Kreysa. Springer, n.d. Web. 09 Sept. 2013.
4. Sumikura, Seiichi, Shogo Mori, Shinya Shimizu, Hisanao Usami, and Eiji Suzuki. "Syntheses of NiO Nanoporous Films Using Nonionic Triblock Co-polymer Templates and Their Application to Photo-cathodes of P-type Dye-sensitized Solar Cells." *Journal of Photochemistry and Photobiology A: Chemistry* 199.1 (2008): 1-7. Print.
5. Ye, Yin, Fangli Yuan, and Shaohua Li. "Synthesis of CoO Nanoparticles by Esterification Reaction under Solvothermal Conditions." *Materials Letters* 60.25-26 (2006): 3175-178. Print.
6. Zheng, Mingtao, Haoran Zhang, Xuebin Gong, Ruchun Xu, Yong Xiao, Hanwu Dong, Xiaotang Liu, and Yingliang Liu. "A Simple Additive-free Approach for the Synthesis of Uniform Manganese Monoxide Nanorods with Large Specific Surface Area." *Nanoscale Research Letters* 8.1 (2013): 166. Print.
7. Chiba, Yasuo, Ashraful Isham, Yuki Watanabe, Ryoichi Komiya, Naoke Koide, and Liyuan Han. "Dye-Sensitized Solar Cells with Conversion Efficiency of 11.1%." *Japanese Journal of Applied Physics* 45.25 (2006): n. pag. Web.
8. Shriver, D. F., P. W. Atkins, and Cooper Harold Langford. *Inorganic Chemistry*. New York: Freeman, 1990. Print.
9. Jahn-Teller Distortions." UC Davis - Chemwiki. University of California, Davis, n.d. Web. 05 Apr. 2014.<http://chemwiki.ucdavis.edu/Inorganic_Chemistry/Coordination_Chemistry/Coordination_Numbers/Jahn-Teller_Distortions>.

10. Shiyu Chen, Lin-Wang Wang "Thermodynamic Oxidation and Reduction Potentials of Photocatalytic Semiconductors in Aqueous Solutions." *Chemistry of Materials* 24 (2012): 3659-3666
11. He, Mingfu, Zhiqiang Ji, Zhongjie Huang, and Yiying Wu. "Molecular Orbital Engineering of a Panchromatic Cyclometalated Ru(II) Dye for P-Type Dye-Sensitized Solar Cells." *The Journal of Physical Chemistry* (2014): n. pag. Web.
12. Qin, Peng, Hongjun Zhu, Tomas Edvinsson, Gerrit Boschloo, Anders Hagfeldt, and Licheng Sun. "Design of an Organic Chromophore for P-Type Dye-Sensitized Solar Cells." *Journal of the American Chemical Society* 130.27 (2008): 8570-571. Print.

Appendix A: XRD

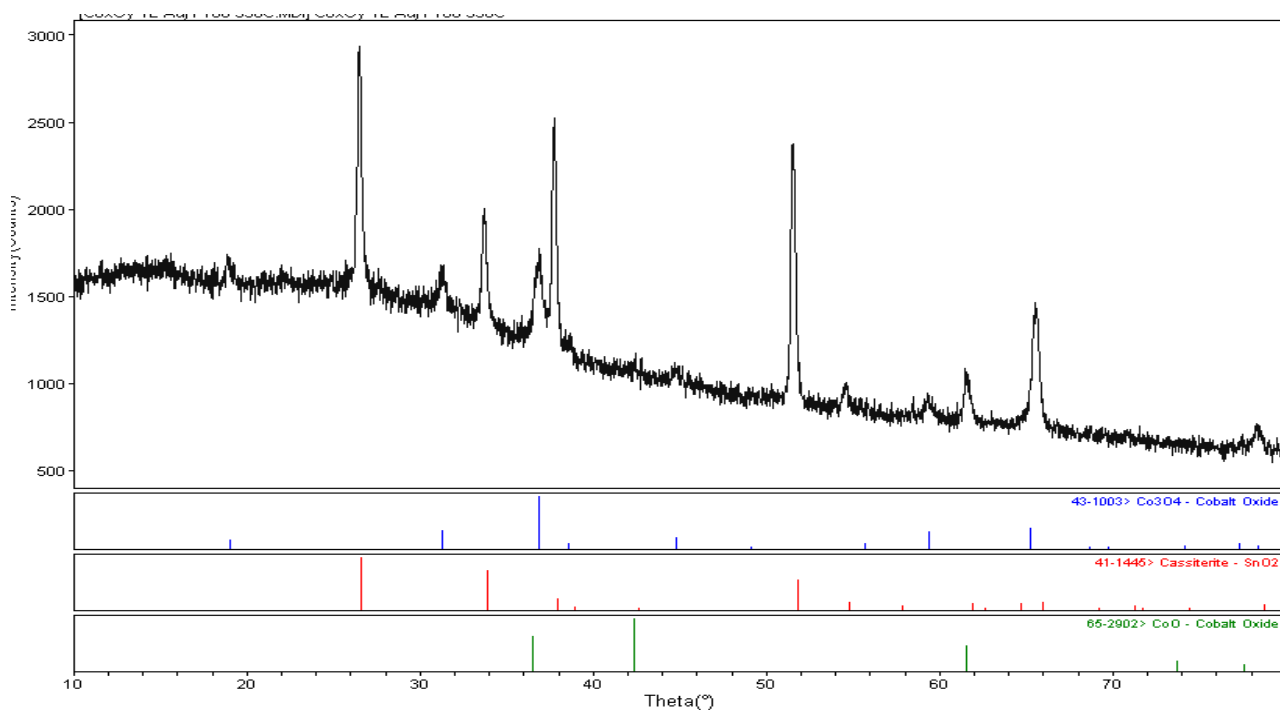


Figure A1: XRD of Co_3O_4 (350°C) Film

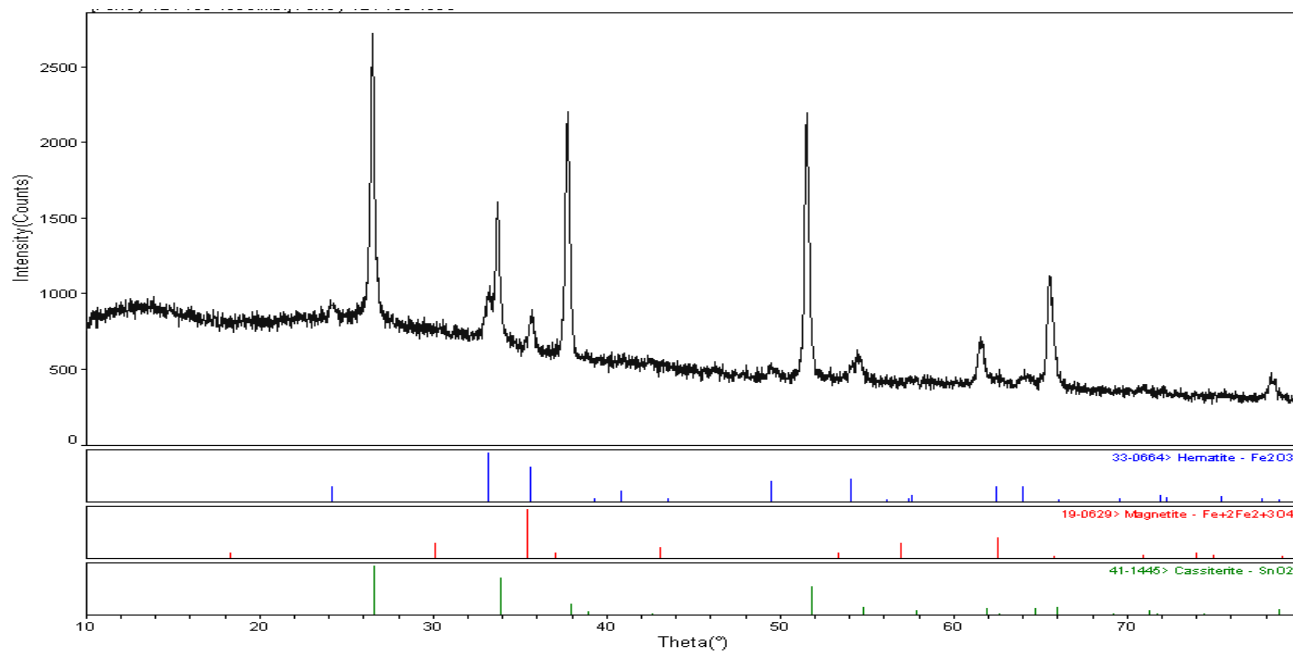


Figure A2: XRD of Fe_2O_3 (450°C) Film

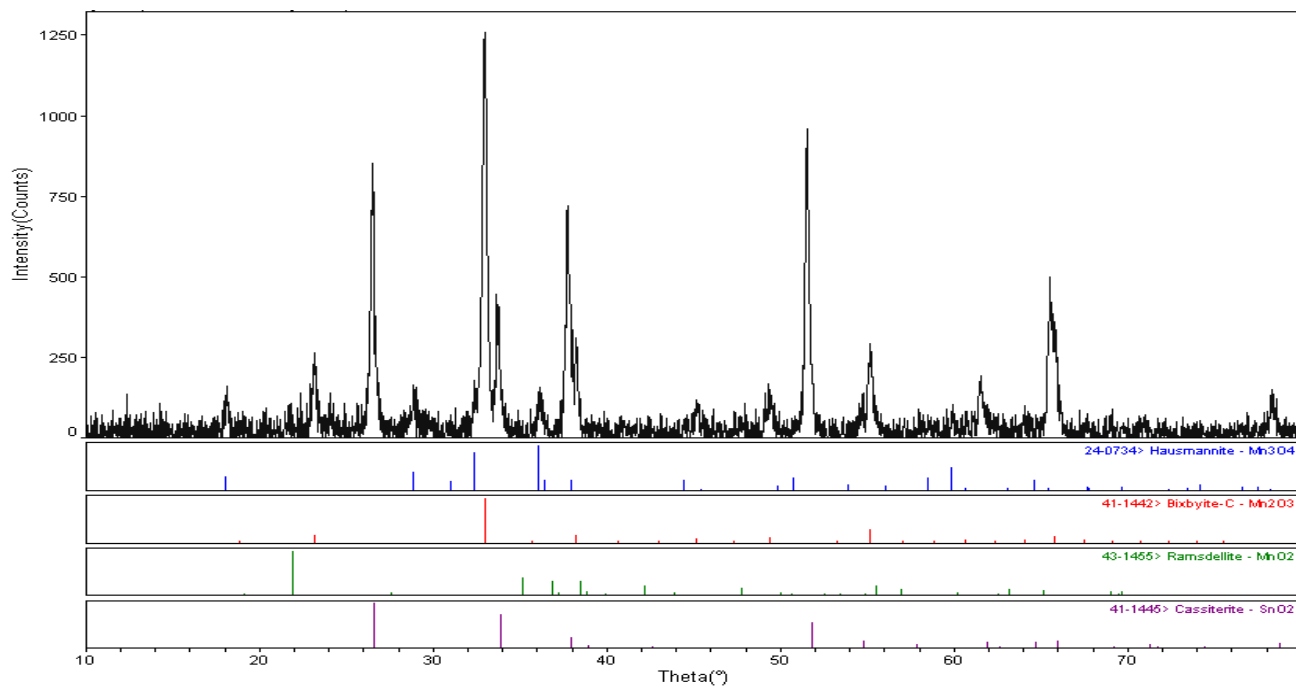


Figure A3: XRD of $\text{Mn}_3\text{O}_4/\text{Mn}_2\text{O}_3$ (450°C) Film

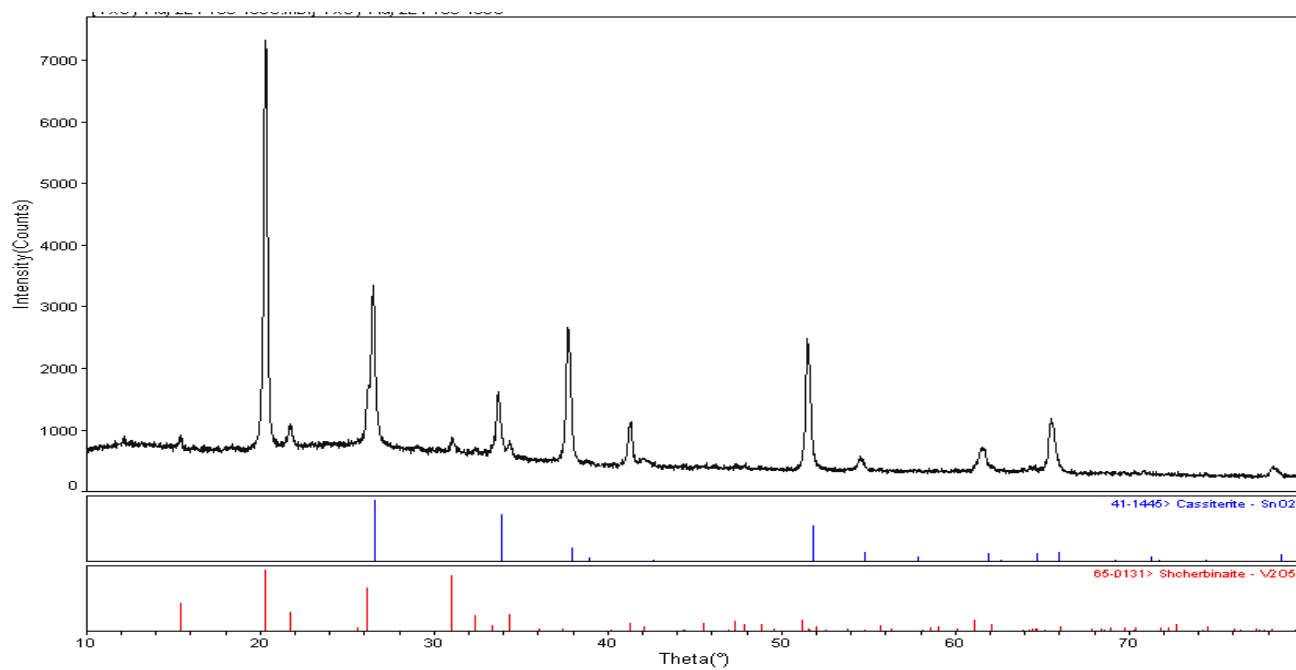


Figure A4: XRD of V_2O_5 (450°C) Film

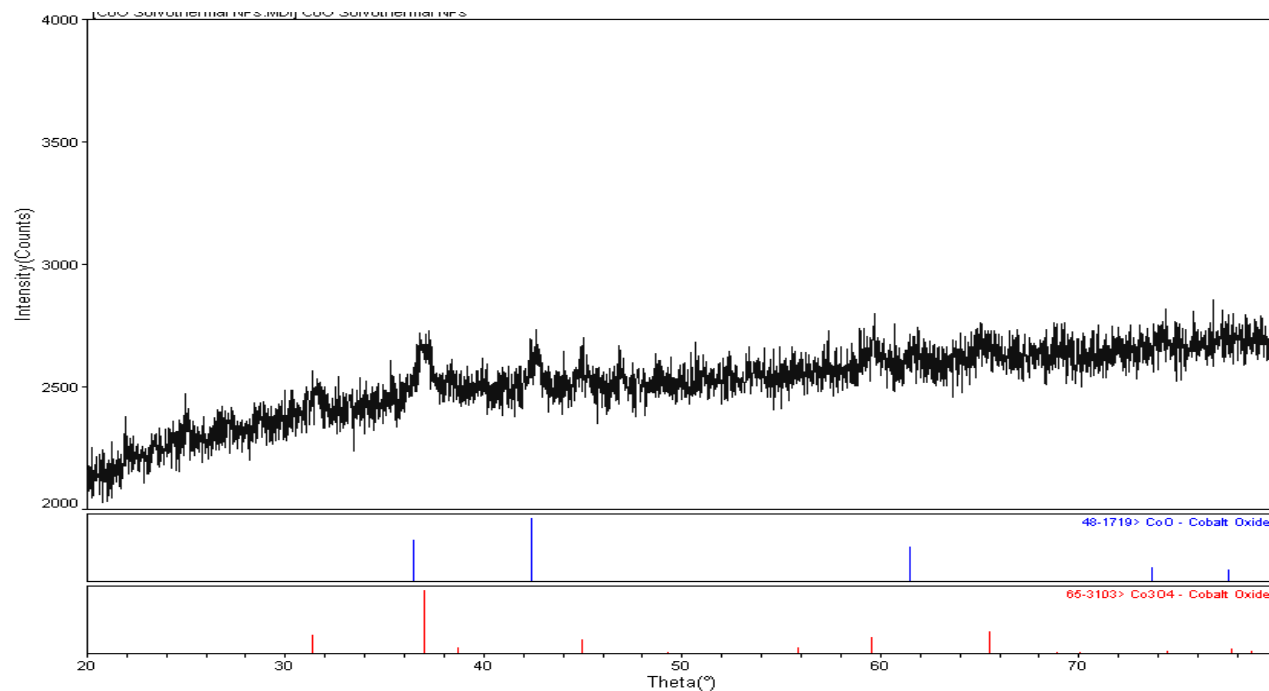


Figure A5: XRD of CoO precipitate

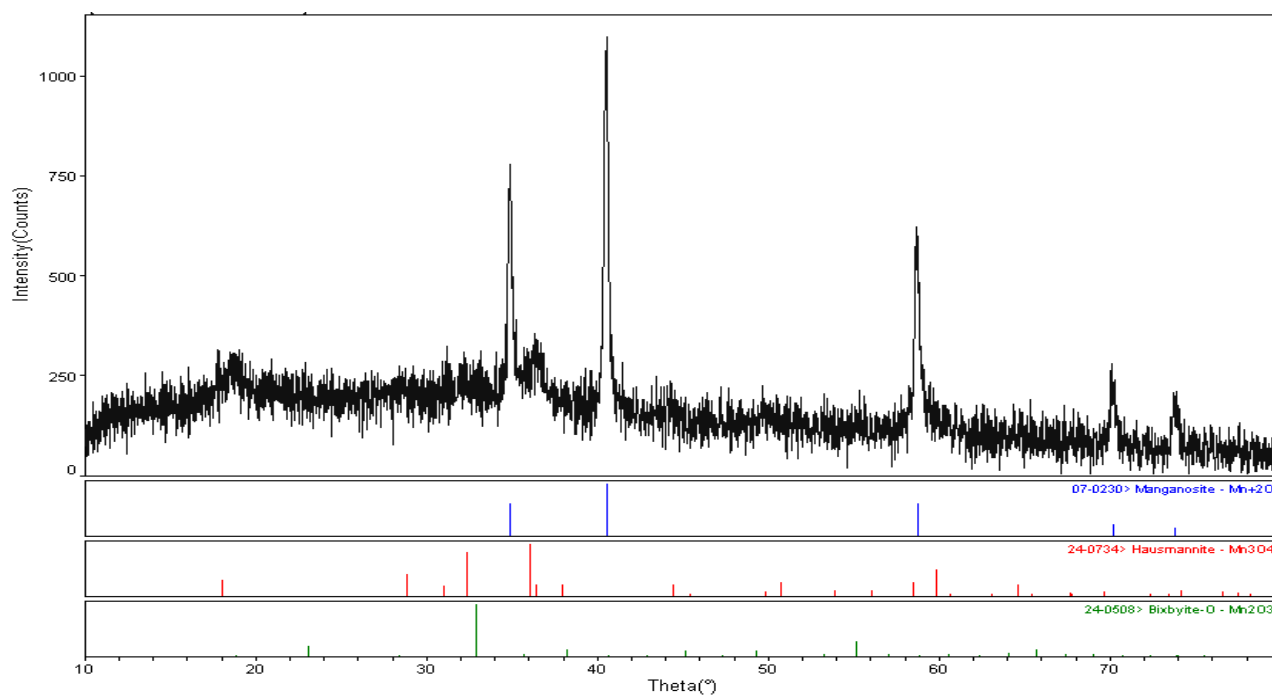


Figure A6: XRD of MnO Precipitate

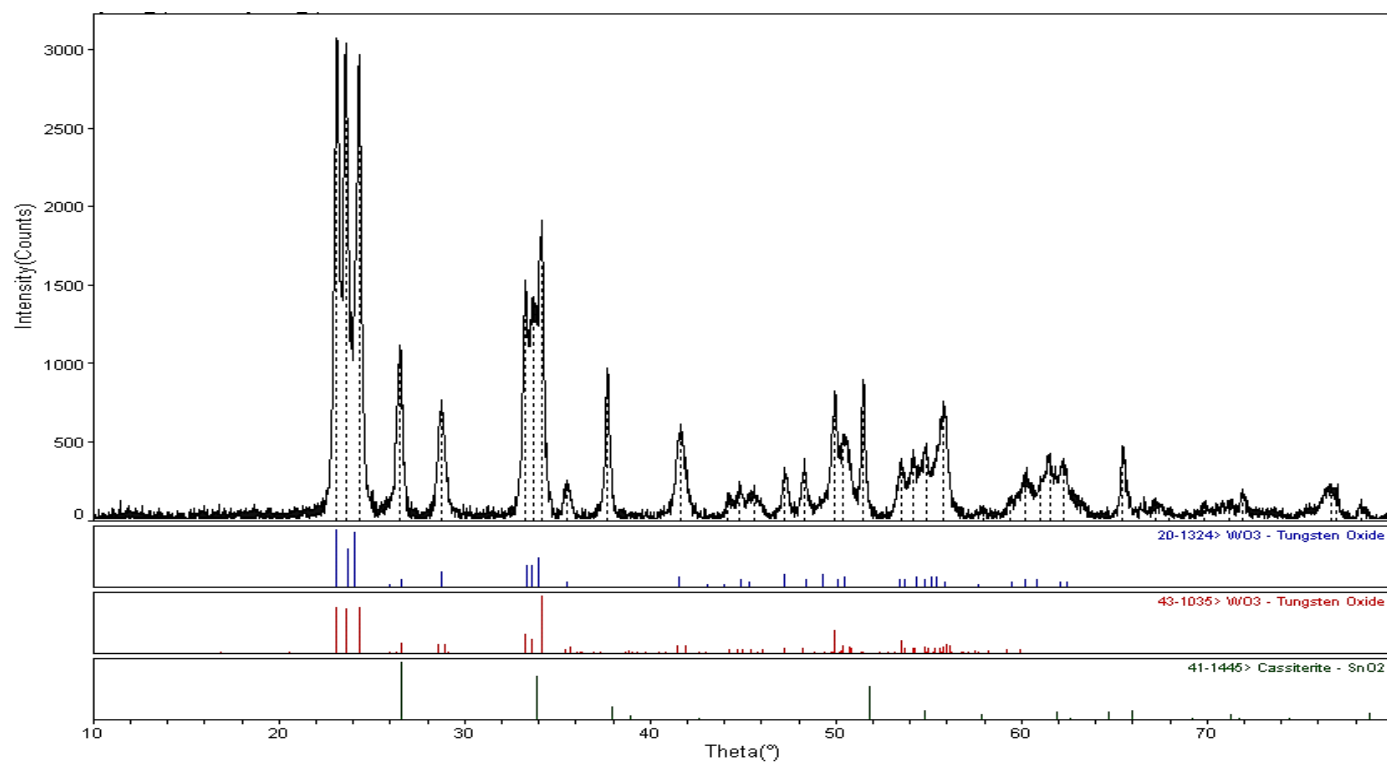


Figure A7: XRD of WO_3 Precipitate

Appendix B: Cyclic Voltammetry

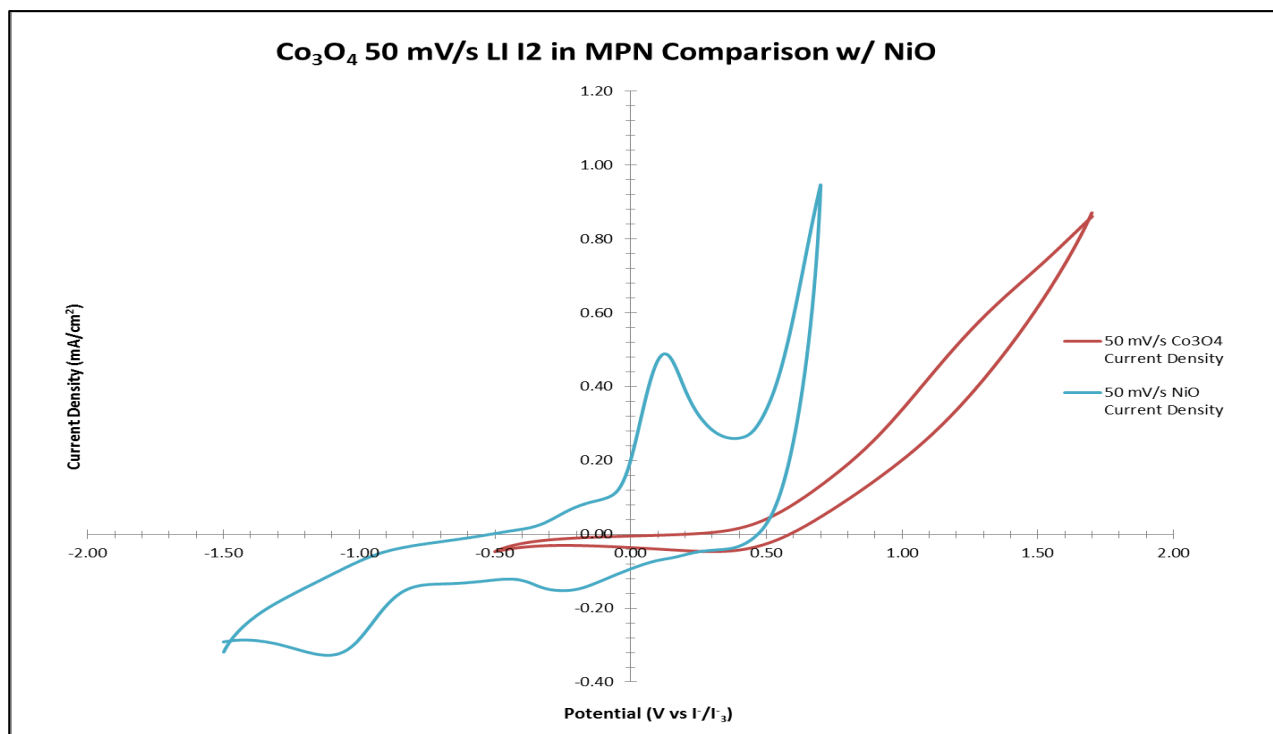


Figure B1: CV of CO3O4

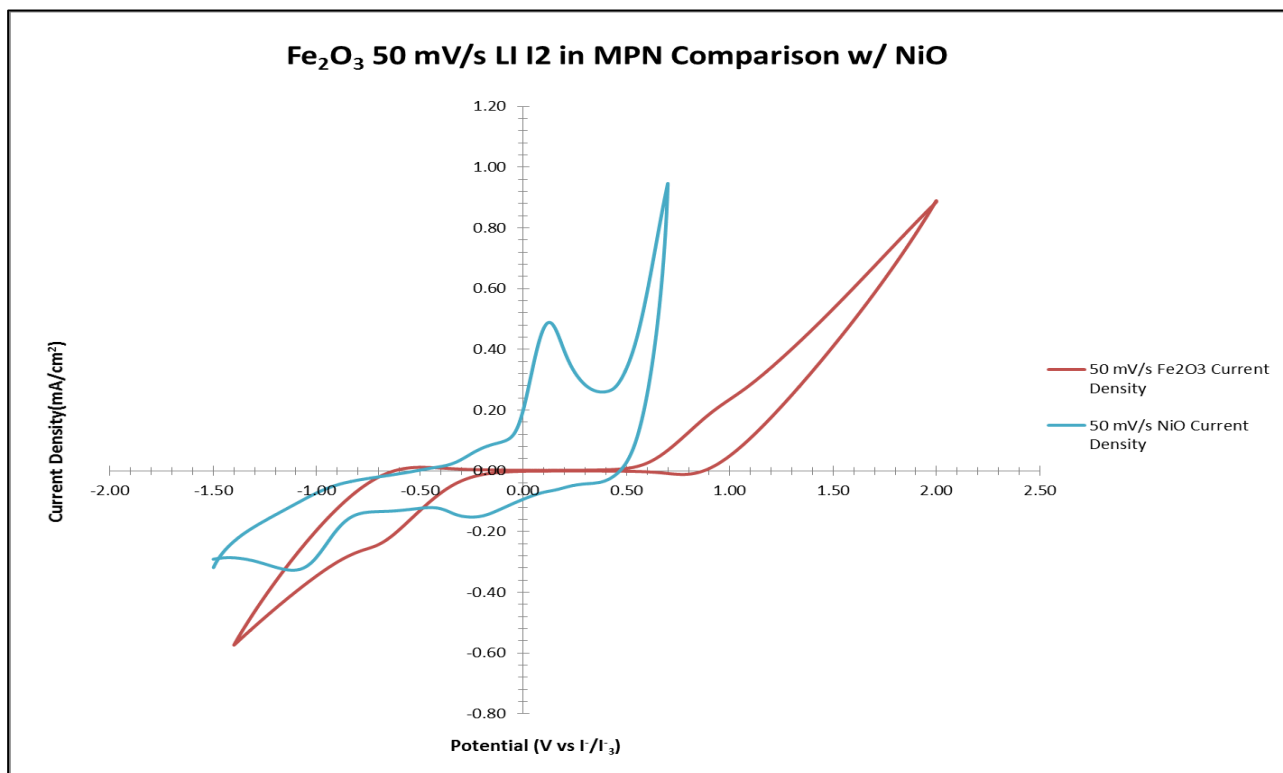


Figure B2: CV of Fe₂O₃

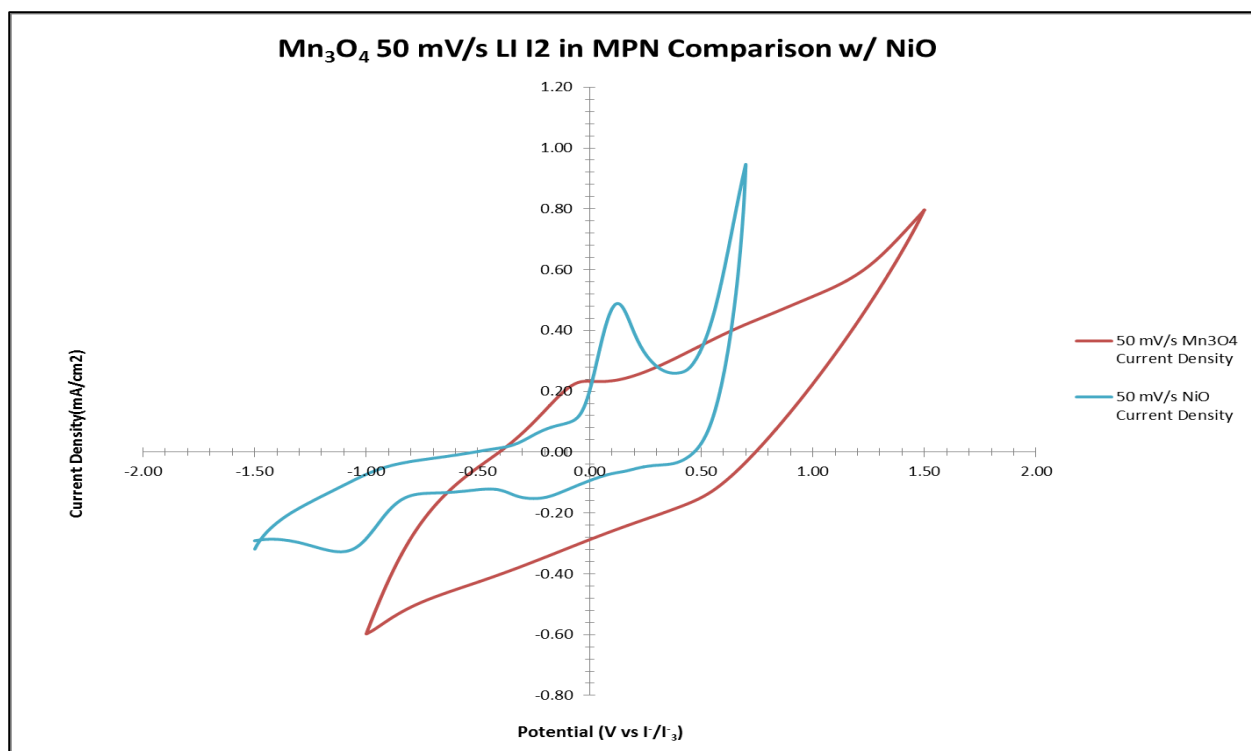


Figure B3: CV of Mn₃O₄

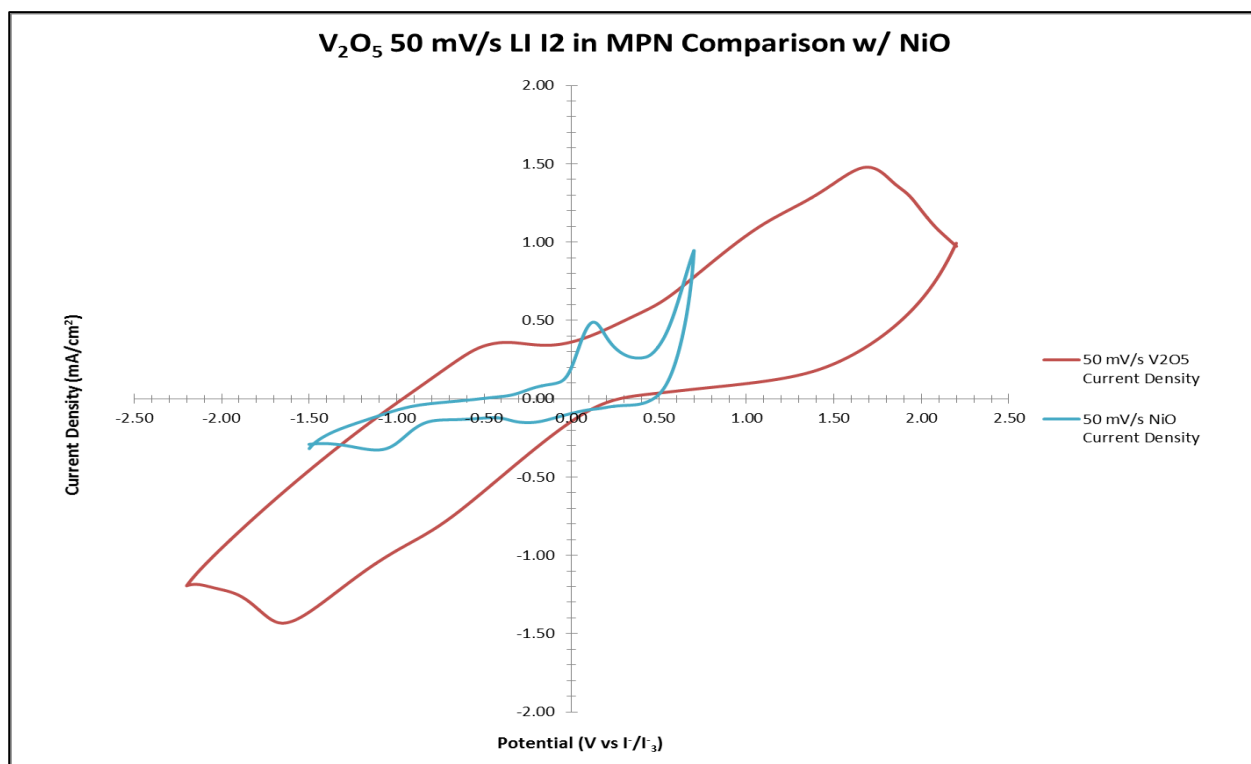


Figure B4: CV of V₂O₅